ISSN(Online) : 2319-8753
ISSN (Print) : 2347-6710

International Journal of Innovative Research in Science, Engineering and Technology

(An ISO 3297: 2007 Certified Organization)

Vol. 5, Issue 9, September 2016

Alternate Arm Converter with MMC

Yashoda.R.Perkar[1], K.V.Ramamohan[2]

P.G. Student, Department of Electrical Engineering, MSS''s College of Engineering and Technology, Jalna, India

Asst. professor, Department of Electrical Engineering, MSS's College of Engineering and Technology Jalna, India

ABSTRACT: A new operating mode of the Modular Multilevel Converter (MMC) using modified arm current waveforms inspired from the working principle of the Alternate Arm Converter (AAC) is presented in this paper. A reduction in the cell voltage deviation is observed at power factors close to unity at the cost of an increase in power losses, especially when reactive power is required. This gain in voltage margin is then used in further optimizations of the MMC performance, mainly focusing on either increasing the number of redundant cells or improving the overall power efficiency of the converter.

KEYWORDS: AC–DC power converters, emerging topologies, fault tolerance, HVDC transmission, multilevel converters, power system faults, STATCOM

I. INTRODUCTION

The Modular Multilevel Converter (MMC), illustrated in Fig. 1, was the first modular Voltage Source Converter (VSC) to provide both low switching losses and low AC current distortion; these features contribute to the higher power efficiency and the significant reduction in the size of the AC filters of recent VSC power stations. A number of MMC converter stations are now in operation and more are planned in the next couple of years with power ratings ever increasing. Over the last few years, a new family of hybrid topologies, such as the Alternate Arm Converter (AAC), drawn in Fig. 2, has emerged.

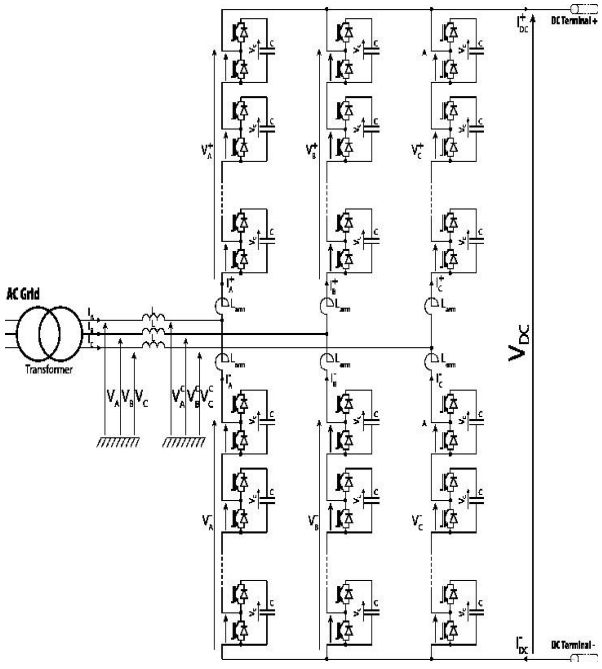

Figure 1 - Half-bridge MMC topology

ISSN(Online) : 2319-8753
ISSN (Print) : 2347-6710

International Journal of Innovative Research in Science, Engineering and Technology

(An ISO 3297: 2007 Certified Organization)

Vol. 5, Issue 9, September 2016

These topologies essentially combine both the 2-level VSC and the MMC together in order to improve on some characteristics such as smaller overall volume, better power efficiency and, in some topologies, DC-side fault blocking capability. It has also been shown that the AAC has a better temperature distribution between the IGBT modules of a cell in comparison to the MMC. Extensive studies have also presented different modeling approaches of the electrical dynamics of these multilevel converters and it has been shown that reduced dynamic models have an acceptable level of accuracy while offering an appreciable boost in computing speed.

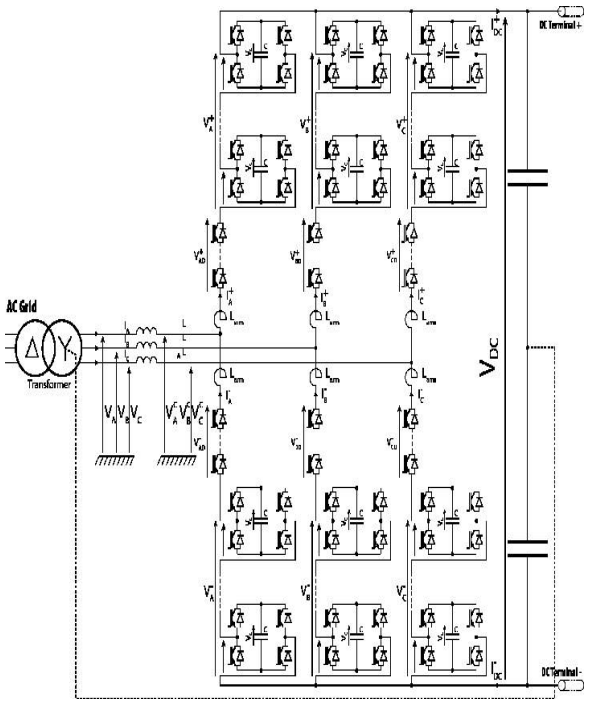

Figure 2 - AAC topology

The AAC has a relatively similar electrical topology to the MMC with the main difference being the presence of director switches, i.e. series-IGBTs, in its arms in series with the stack of cells. The switching state of these director switches determines which arms are both generating the converter voltage waveform and carrying the AC current to the respective DC terminal. This approach has proven, to be both power and volume effective, resulting in (i) the number of cells be significantly reduced, e.g. up to half the number of cells compared to the MMC, (ii) the average cell voltage deviation is lower allowing smaller capacitors in the cells and (iii) the use of full H-bridge cells instead of half-bridge cells, thus the AAC is able to block DC-side faults without compromising its overall power efficiency.

In the case of the MMC, it was observed rapidly after the topology was proposed that unplanned circulating currents were running between the legs. This issue was later solved by implementing additional feedback loops in charge of monitoring the arm currents. Besides, it has also been observed that this circulating current can be used to reduce the cell voltage deviation of the cell capacitor or by adding a 2nd harmonic filter at the midpoint of the arm inductors. This paper presents an original arm current waveform for the in the MMC, inspired by the working mechanism of the AAC. This study focuses on the effects of changing the arm current waveforms which only implies an update of the control system (software) but not the converter itself (hardware) which thus stays the same.

This implies that (i) both the AC and DC quantities (e.g. power, voltage and current magnitudes) remain unchanged, (ii) the cells are still of the half-bridge type and (iii) the passive components (e.g. cell capacitors and arm inductors) keep the same values. Furthermore only the top level part of the controller is affected but the low-level control stays the same thus this does not require changes in either the wiring or the communication with the cells. Finally the benefits of

ISSN(Online) : 2319-8753
ISSN (Print) : 2347-6710

International Journal of Innovative Research in Science, Engineering and Technology

(An ISO 3297: 2007 Certified Organization)

Vol. 5, Issue 9, September 2016

this update both in terms of cell capacitor voltage deviation and power efficiency will be explored and margins for further optimizations are discussed. Finally, modular VSC topologies such as the MMC and the AAC can also be connected in front-to-front arrangements (meaning that the AC sides are facing each others) in order to form a DC/DC converter. Therefore the current modulation concept introduced in this paper can potentially also be used in such DC/DC topologies with equivalent pros and cons as discussed in this paper.

II. ARM CURRENT WAVEFORMS

In its classic operating mode, the MMC distributes equally (i) the AC current between its upper and lower arms and (ii) the DC current between the three different legs. The complete set of equations describing the arm currents is given in (1)-(6). The signs present in these equations depend on the direction of the currents, using what is illustrated in Fig 1 and 2

$$I_{A+} = I_{A}/2 + I_{DC}/3 \quad (1)$$
$$I_{A-} = -I_{A}/2 + I_{DC}/3 \quad (2)$$
$$I_{B+} = I_{B}/2 + I_{DC}/3 \quad (3)$$
$$I_{B-} = -I_{B}/2 + I_{DC}/3 \quad (4)$$
$$I_{C+} = I_{C}/2 + I_{DC}/3 \quad (5)$$
$$I_{C-} = -I_{C}/2 + I_{DC}/3 \quad (6)$$

The AAC distributes its AC currents in a different pattern as only one arm in each leg carries the full AC current while the other has its director switch opened, blocking any current from flowing through the arm. Using the variables $\alpha_{A,B,C} \in \{0,1\}$ which represent whether the AC current of a particular leg is passing either through the top or bottom arm, the set of equations describing the arm currents in AAC mode are given in (7)-(12):

$$I_{A+} = \alpha_A I_A - I_F/3 \quad (7)$$
$$I_{A-} = -(1-\alpha_A) I_A - I_F/3 \quad (8)$$
$$I_{B+} = \alpha_B I_B - I_F/3 \quad (9)$$
$$I_{B-} = -(1-\alpha_B) I_B - I_F/3 \quad (10)$$
$$I_{C+} = \alpha_C I_C - I_F/3 \quad (11)$$
$$I_{C-} = -(1-\alpha_C) I_C - I_F/3 \quad (12)$$

However the AAC inherently generates a 6-pulse ripple on top of the DC current waveform as a consequence of the alternating nature of the arm conduction periods. Since the objective of this study is to migrate an already existing MMC converter to an AAC mode of operation without having to change the hardware but only by updating the control system (i.e. software), installing a DC filter is out of question. To resolve this issue, an additional active filtering current is added to the arm currents in order to keep the DC current smooth. This filtering current I_F (13) is obtained by calculating the ripple component of the DC current waveform resulting from AAC operation in order to suppress it by adding a circulating current of opposing sign through all three legs.

$$\begin{aligned} I_F &= I_{A+} + I_{B+} + I_{C+} - I_{DC} \\ &= I_{A-} + I_{B-} + I_{C-} - I_{DC} \\ &= \alpha_A I_A + \alpha_B I_B + \alpha_C I_C - I_{DC} \end{aligned} \quad (13)$$

The addition of this active filtering current alters the original nature of the AAC mode as the arms will now continuously run a current through them as opposed to for only one half of the cycle and no current during the other half of the cycle because the director switches would be closed. However the magnitudes of the arm currents will be small for a large proportion of the time, while the arm is not carrying the main AC current, compared to the MMC mode of operation, as shown in the simulation section below. Finally, only the arm current waveform will be different because the currents seen at both the AC and DC terminals of the converter will be the same as under the normal MMC mode of operation.

ISSN(Online) : 2319-8753
ISSN (Print) : 2347-6710

International Journal of Innovative Research in Science, Engineering and Technology

(An ISO 3297: 2007 Certified Organization)

Vol. 5, Issue 9, September 2016

III. SIMULATION

A. SIMULATION MODEL

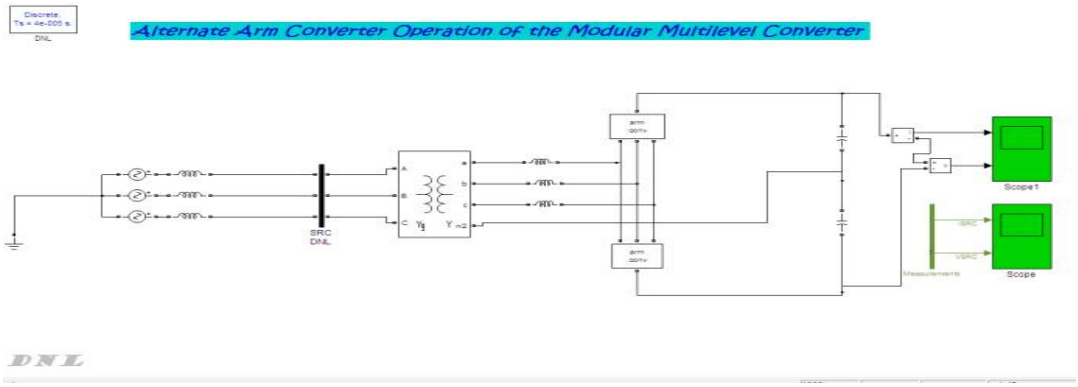

Fig.3- Optimization Scenarios Matlab model

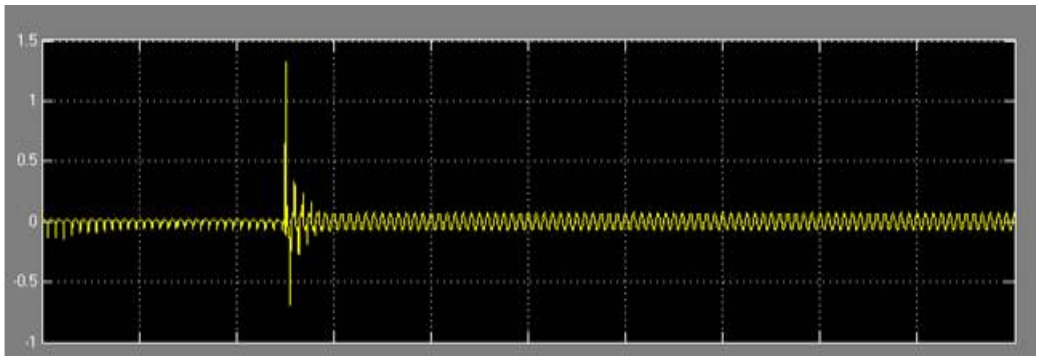

Fig.4-Arm converter outputs for current

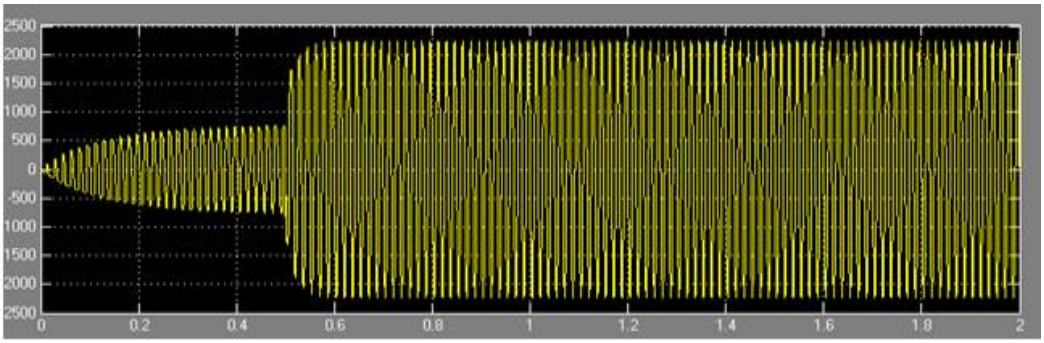

Fig: Arm converter output for voltage

ISSN(Online) : 2319-8753
ISSN (Print) : 2347-6710

International Journal of Innovative Research in Science, Engineering and Technology

(An ISO 3297: 2007 Certified Organization)

Vol. 5, Issue 9, September 2016

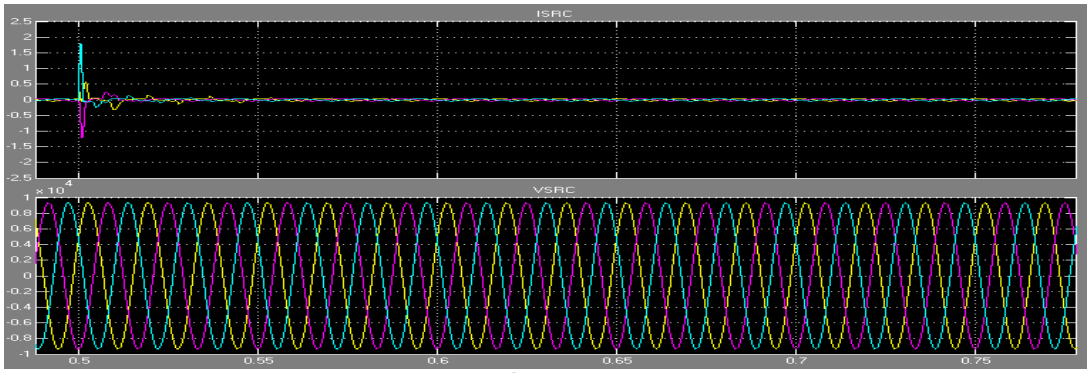

Fig.5- Source outputs

In order to assess the benefits of the AAC mode of operation, shown in fig.3 a 120 MW MMC converter has been simulated using Simulink® and the Artemis® toolbox in order to simulate a reasonably large number of half-bridge cells. The characteristics of this simulation model are listed in Table 1. In order to better match realistic MMC converter, triplen harmonic voltage injection has been used (about 15% of the fundamental magnitude) in order to shape the converter voltage waveform into an almost trapezoidal waveform and to push the power rating to its theoretical maximum while still using only half-bridge cells. Furthermore, a power loss analysis has also been performed by post-processing the voltage and current waveforms in each cells using the power loss data from the datasheet of the 3.3 kV 1.2 kA HiPak IGBT device 5SNA 1200E330100. In the later part of the simulation section, the steady state junction temperature of the different semiconductor devices in a cell (e.g. top and bottom IGBT and diode modules) by applying the individual power loss figure of each device into a power-thermal model derived in ANSIS and assuming a coolant temperature of 60ºC shared by all the semiconductor devices.

Table 1 - Characteristics of the simulated MMC model

Rated power	120 MW
DC bus	±50 kV
AC line	55 kV
AC frequency	50 Hz
Triplen harmonic voltage	15%
Number of cells per stack	56
Cell capacitor	8 mF
Phase inductor	8 mH
Arm inductor	6 mH

ISSN(Online) : 2319-8753
ISSN (Print) : 2347-6710

International Journal of Innovative Research in Science, Engineering and Technology

(An ISO 3297: 2007 Certified Organization)

Vol. 5, Issue 9, September 2016

B. ARM CURRENT WAVEFORMS

The arm current waveforms resulting from this mode of operation are observed in this section. Fig. 6 shows the top arm current waveform in both MMC and AAC operating modes (respectively the red and green curves) under unity power factor rectifier mode. The third curve (blue) is the result of the difference between the two waveforms and can be interpreted as the equivalent circulating current which can be injected in the converter to move from the MMC mode to the AAC mode of operation. It can be observed that at unity power factor a large amount of the fundamental cycle is spent with a small amount of current magnitude in AAC mode as opposed to the MMC mode. As more reactive power is involved in the conversion process as shown in Fig 7 (same amount of active and reactive power) and in Fig. 8 (reactive power only), the arm current waveform becomes more and more distorted in AAC mode with still a significant portion of the cycle used by low magnitude current but at the expense of an increasing peak values to attain twice the value in the MMC mode. The power losses have computed for different operating points and the results listed in Table 2 with the total power loss values plotted in accordance to the angular value of their respective operating points in Fig. 9.

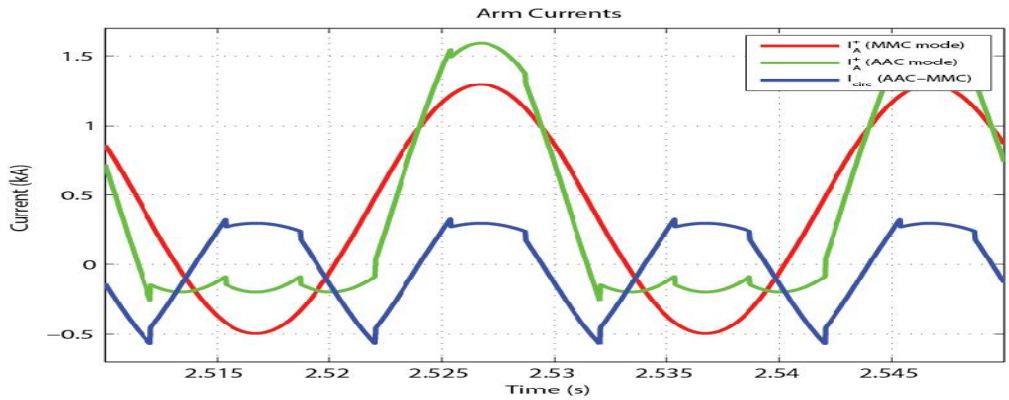

Figure 6 - Arm A+ current waveform in MMC (red), AAC (green) modes and the resulting circulating current (blue) with active power only

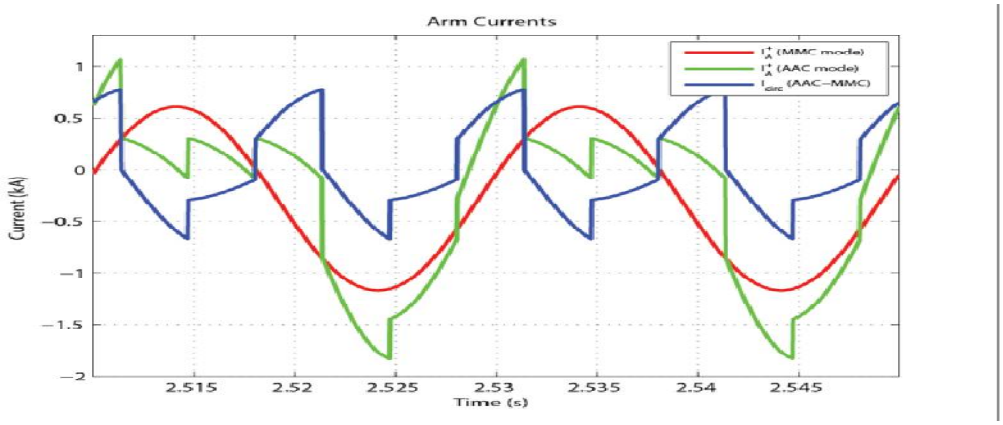

Figure 7 - Arm A+ current waveform in MMC (red), AAC (green) modes and the resulting circulating current (blue) with both active and reactive powers

ISSN(Online) : 2319-8753
ISSN (Print) : 2347-6710

International Journal of Innovative Research in Science, Engineering and Technology

(An ISO 3297: 2007 Certified Organization)

Vol. 5, Issue 9, September 2016

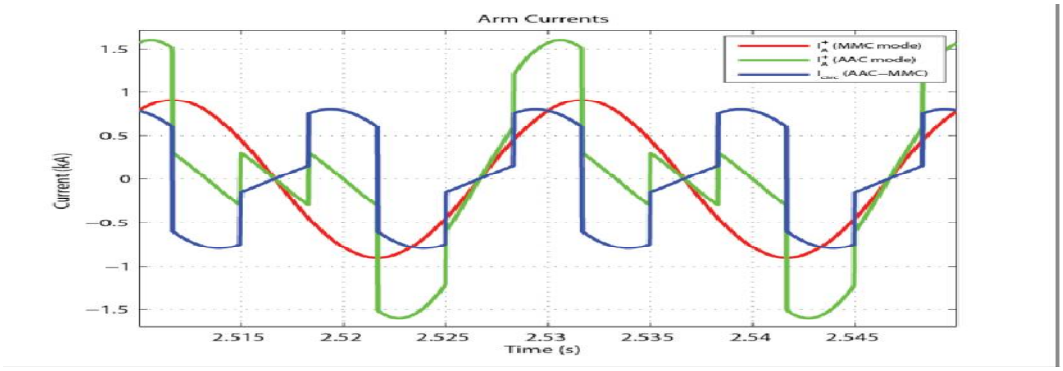

Figure 8 - Arm A+ current waveform in MMC (red), AAC (green) modes and the resulting circulating current (blue) with reactive power only

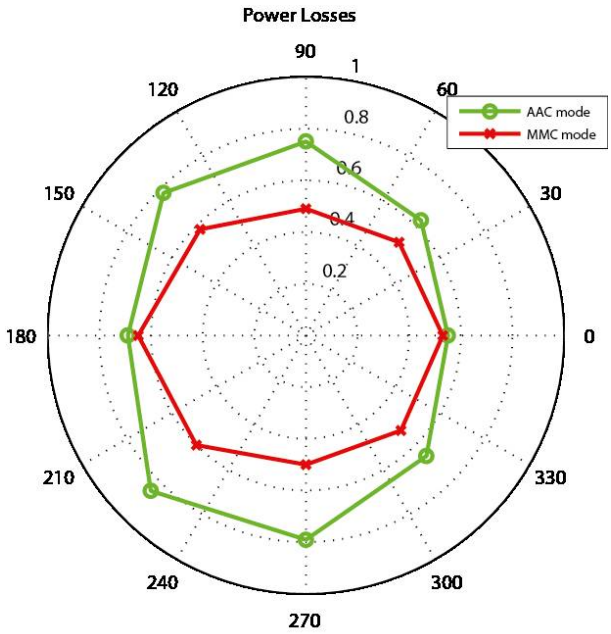

Figure 9 - Power losses as percent of the total apparent power in MMC and AAC modes for different operating points

ISSN(Online) : 2319-8753
ISSN (Print) : 2347-6710

International Journal of Innovative Research in Science, Engineering and Technology

(An ISO 3297: 2007 Certified Organization)

Vol. 5, Issue 9, September 2016

Table 2 – Power losses of the MMC model depending on the mode of operation and operating point relative to the apparent power

Active Power Reactive Power		1 pu 0 pu	0.7pu 0.7 pu	0 pu 1 pu	-0.7pu 0.7 pu	-1 pu 0 pu	-0.7pu -0.7pu	0 pu -1 pu	0.7pu -0.7pu
MMC mode	Conduction losses	0.50%	0.44%	0.36%	0.37%	0.38%	0.37%	0.35%	0.45%
	Switching losses	0.15%	0.14%	0.13%	0.13%	0.15%	0.15%	0.15%	0.16%
	Total losses	0.65%	0.58%	0.49%	0.51%	0.53%	0.52%	0.50%	0.60%
AAC mode	Conduction losses	0.53%	0.56%	0.51%	0.43%	0.38%	0.40%	0.49%	0.53%
	Switching losses	0.16%	0.22%	0.24%	0.20%	0.17%	0.26%	0.30%	0.32%
	Total losses	0.69%	0.78%	0.75%	0.63%	0.55%	0.66%	0.79%	0.85%

C. OBSERVATION AT UNITY POWER FACTOR

The previous set of results indicates that this new AAC mode is only potentially attractive for unity power factor only as both the arm current peak values and the power losses are increase dramatically when reactive power is involved in the conversion process. The next part of this paper assumes that only these two operating points (inverter and rectifier active power only) are considered with the results focusing on the rectifier mode mainly since the inverter mode is merely an opposite phase angle version of the former.

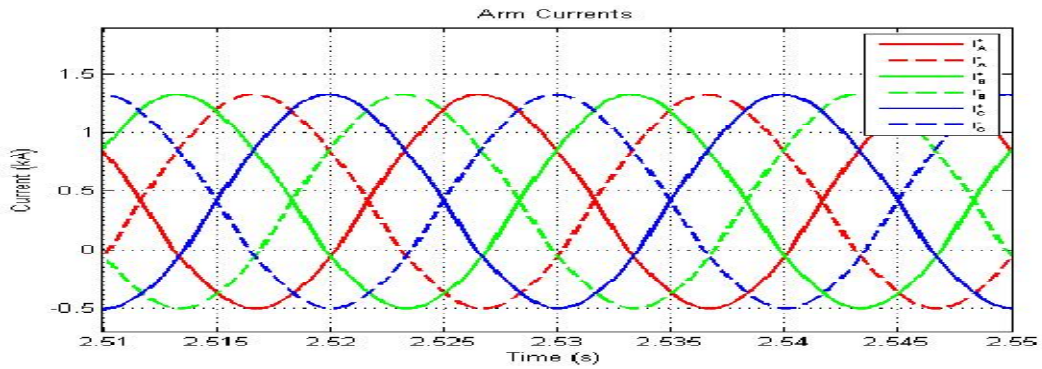

Figure 10- Arm current waveforms in MMC mode

ISSN(Online) : 2319-8753
ISSN (Print) : 2347-6710

International Journal of Innovative Research in Science, Engineering and Technology

(An ISO 3297: 2007 Certified Organization)

Vol. 5, Issue 9, September 2016

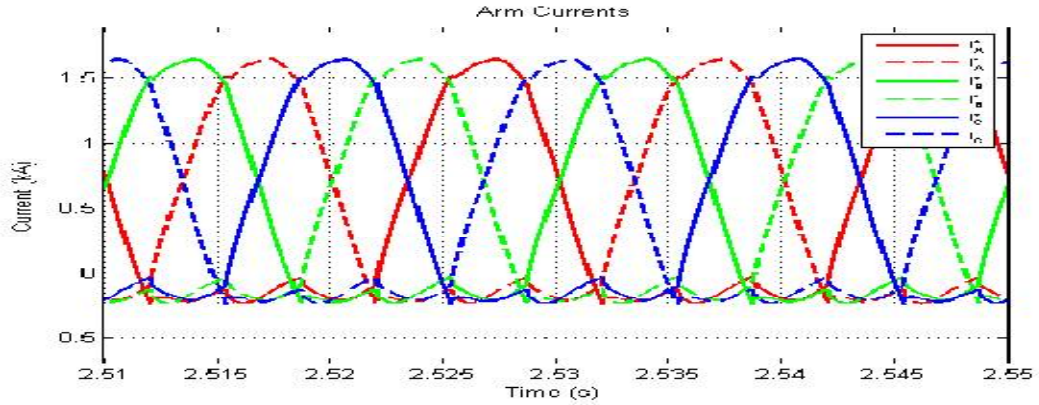

Figure 11 - Arm current waveforms in AAC mode

Fig. 10 and 11 show the arm current waveforms respectively in MMC and AAC modes of operation. On one hand, the MMC mode results in the arms continuously conducting a large amount of current as opposed to the AAC mode where a significant part of the cycle is spent with only a small amount of current (around -150 A). This remaining low magnitude current mainly consists of the filtering current I_F (13). On the other hand, the peak value of the arm current currents is lower in the MMC mode compared to the AAC mode (respectively 1.3 kA and 1.6 kA thus 23% higher in the AAC case).

IV. CONCLUSION

The AAC mode of operation of an existing MMC station has been presented in this paper. This new mode of operation does not require any hardware modification of the converter station but rather an update of the control system, hence mainly software. Generally the power losses increase in the AAC mode of operation compared to the MMC mode but are approximately the same when operating close to unity power. Given this fact, the study focused only on active power conversion operating points. In this condition, the AAC-mode still exhibits higher peak arm current combined with a significant part of the cycle at low current magnitudes but, most importantly, smaller cell voltage deviations (e.g. 30% lower) compared to the classic MMC mode are observed.

This last fact can be used to further optimize the performance of the MMC converter station in two different ways. First, reducing the switching frequency of the PWM signal will result in a substantial decrease in the switching losses, hence a higher power efficiency figure for the converter station. This leads also to an increase of the individual cell voltage deviations but those are still contained within the same limits set during the previous MMC mode. Second, increasing slightly the nominal voltage of the cells results in having some cells being made redundant (approximately 5% of the cells in each stack) since the stacks are able to produce more voltage than normally required. Despite the higher nominal voltage, the maximum peak value hit by the cell voltages is still the same maximum value set during the previous MMC mode of operation. From here, either (i) these redundant cells are electrically bypassed in order to further improve the power efficiency of the converter station, or (ii) they can be used as back-up cells in case of other cell failures, thus further improving the overall reliability of the MMC.

ACKNOWLEDGMENT

I would like to express my special thanks of gratitude to my PG guide Prof. K. V. Ramamohan sir as well as our principle Dr. C. M. Sedani sir who gave me the golden opportunity to do this wonderful project on the topic Alternate Arm Converter with MMC. Which also helped me in doing a lot of Research and I came to know about so many new things I am really thankful to them. I sincerely thank to all my faculty members of MSS's collage of engineering and technology, jalna for their continues encouragement and active interest in my progress that they gave throughout the work.

ISSN(Online) : 2319-8753
ISSN (Print) : 2347-6710

International Journal of Innovative Research in Science, Engineering and Technology

(An ISO 3297: 2007 Certified Organization)

Vol. 5, Issue 9, September 2016

REFERENCES

[1] D. R. Trainer, C. C. Davidson, C. D. M. Oates, N. M. MacLeod, D. R. Critchley, and R. W. Crookes, "A new hybrid voltage-sourced converter for HVDC power transmission," CIGRE Paris Sess. 2010, 2010.
[2] A. Lesnicar and R. Marquardt, "An innovative modular multilevel converter topology suitable for a wide power range," in Power Tech Conference Proceedings, 2003 IEEE Bologna, vol. 3, june 2003
[3] Sellick, R. L., and M. Åkerberg. "Comparison of HVDC Light (VSC) and HVDC Classic (LCC) Site Aspects, for a 500MW 400kV HVDC Transmission Scheme." AC-DC 2012, Birmingham UK.
[4] Merlin, M.M.C.; Green, T.C.; Mitcheson, P.D.; Trainer, D.R.; Critchley, R.; Crookes, W.; Hassan, F., "The Alternate Arm Converter: A New Hybrid Multilevel Converter With DC-Fault Blocking Capability," Power Delivery, IEEE Transactions on , vol.29, no.1, pp.310-317, Feb. 2014.
[5] Adam, Grain Philip, et al. "New breed of network fault-tolerant voltage-source-converter HVDC transmission system." Power Systems, IEEE Transactions on 28.1 (2013): 335-346.

BIOGRAPHY

Miss. Yashoda Rambhau Perkar was received the B.E. degree in Electrical Electronics and Power from PESCOE (Dr. BAMU) Aurangabad in 2013 and pursuing M.E. in Electrical Power System from MSSCET (Dr. BAMU, Aurangabad), Jalna.

Prof. K. V. Ramamohan was received B-Tech, degree from S.K.T.R.M.C.E. (JNTU) Hyderabad in 2009 and M-Tech from S.P.R.C.E.T.(JNTU) Hydrabad in 2013. Presently he is working as an Asst. professor in the Dept. of Electrical Engineering, from MSS'sCET, Jalna, Maharashtra